



**HAL**  
open science

## Analyzing the anisotropic Hooke s law for children s cortical bone

Emmanuelle Lefèvre, Philippe Lasaygues, Cécile Baron, Cédric Payan, Franck Launay, Hélène Follet, Martine Pithioux

► **To cite this version:**

Emmanuelle Lefèvre, Philippe Lasaygues, Cécile Baron, Cédric Payan, Franck Launay, et al.. Analyzing the anisotropic Hooke s law for children s cortical bone. *Journal of the mechanical behavior of biomedical materials*, 2015, 49, pp.370 - 377. 10.1016/j.jmbbm.2015.05.013 . hal-01167006

**HAL Id: hal-01167006**

**<https://hal.science/hal-01167006>**

Submitted on 23 Jun 2015

**HAL** is a multi-disciplinary open access archive for the deposit and dissemination of scientific research documents, whether they are published or not. The documents may come from teaching and research institutions in France or abroad, or from public or private research centers.

L'archive ouverte pluridisciplinaire **HAL**, est destinée au dépôt et à la diffusion de documents scientifiques de niveau recherche, publiés ou non, émanant des établissements d'enseignement et de recherche français ou étrangers, des laboratoires publics ou privés.

# Analyzing the anisotropic Hooke's law for children's cortical bone

Emmanuelle Lefèvre<sup>a,e</sup>, Philippe Lasaygues<sup>b</sup>, Cécile Baron<sup>a,e</sup>, Cédric Payan<sup>b</sup>, Franck  
Launay<sup>a,d</sup>, Hélène Follet<sup>c=</sup>, Martine Pithioux<sup>a,e=</sup>

<sup>a</sup> Aix-Marseille Université, CNRS, ISM UMR 7287, 13288 Marseille cedex 09, France

<sup>b</sup> Laboratory of Mechanics and Acoustics, UPR CNRS 7051, Aix-Marseille University, Centrale Marseille, 13009  
Marseille, France

<sup>c</sup> INSERM, UMR 1033, University of Lyon, 69372 Lyon cedex 08, France

<sup>d</sup> APHM, La Timone, Service de pédiatrie orthopédique, 13385 Marseille cedex 5, France

<sup>e</sup> APHM, Hôpital Sainte-Marguerite, Institute for Locomotion, 13009, Marseille, France

= equal contribution

## Corresponding author:

Emmanuelle Lefèvre

Aix-Marseille Université, CNRS, ISM UMR 7287, 13288 Marseille cedex 09, France

Email address: emmanuelle.lefevre@univ-amu.fr

**Keywords:** *Ultrasonic wave velocities, Stiffness coefficients, Pediatrics, Cortical bone, Anisotropy*

## Abstract

Child cortical bone tissue is rarely studied because of the difficulty of obtaining samples. Yet the preparation and ultrasonic characterization of the small samples available, while challenging, is one of the most promising ways of obtaining information on the mechanical behavior of non-pathological children's bone. We investigated children's cortical bone obtained from surgical waste. 22 fibula or femur samples from 21 children (1-18 years old, mean age:  $9.7 \pm 5.8$  years old) were compared to 16 fibula samples from 16 elderly patients (50-95 years old, mean age:  $76.2 \pm 13.5$  years old). Stiffness coefficients were evaluated via an ultrasonic method and anisotropy ratios were calculated as the ratio of  $C_{33}/C_{11}$ ,  $C_{33}/C_{22}$  and  $C_{11}/C_{22}$ . Stiffness coefficients were highly correlated with age in children ( $R > 0.56$ ,  $p < 0.01$ ). No significant difference was found between  $C_{11}$  and  $C_{22}$  for either adult or child bone ( $p > 0.5$ ), nor between  $C_{44}$  and  $C_{55}$  ( $p > 0.5$ ). We observe a transverse isotropy with  $C_{33} > C_{22} = C_{11} > C_{44} = C_{55} > C_{66}$ . For both groups, we found no correlation between age and anisotropy ratios. This study offers the first complete analysis of stiffness coefficients in the three orthogonal bone axes in children, giving some indication of how bone anisotropy is related to age. Future perspectives include studying the effect of the structure and composition of bone on its mechanical behavior.

## 1. Introduction

Bone is a hierarchical and organized structure with properties varying by successive stages from juvenile to mature state. Numerous studies have aimed to determine the mechanical properties of cortical bone tissue collected from adult human subjects (Bensamoun et al., 2004; Choi et al., 1990;

39 Cuppone et al., 2004; Grimal et al., 2009; Ho Ba Tho et al., 1991; Keller et al., 1990; Lotz et al., 1991;  
40 Reilly et al., 1974; Reilly and Burstein, 1975; Smith and Smith, 1976; Zioupos and Currey, 1998).  
41 Ultrasonic waves have frequently been used in the measurement of the elastic properties of adult bone  
42 *in vitro* (Ashman et al., 1984; Yoon and Katz, 1976; Rho, 1996; Espinoza Orías et al., 2009; Rudy et  
43 al., 2011; Baumann et al., 2012; Bernard et al., 2013). A method based on the measurement of both  
44 longitudinal and shear ultrasonic bulk wave velocities (BWV) allows the determination of numerous  
45 stiffness coefficients of the elasticity tensor  $C_{ijkl}$ , on a single specimen (Ashman et al., 1984; Rho,  
46 1996; Espinoza Orías et al., 2009; Rudy et al., 2011; Baumann et al., 2012; Lang, 1969). Cortical bone  
47 is an anisotropic medium due to its highly oriented, mineralized collagen fibril structure, and the  
48 literature on adults contains different assumptions regarding the type of anisotropy of the cortical bone  
49 structure. Some authors (Haïat et al., 2009; Neil Dong and Edward Guo, 2004; Rho, 1996; Yoon and  
50 Katz, 1976) assume that human cortical bone can be considered as transverse isotropic (five  
51 independent elastic coefficients), meaning that bone elastic properties are similar in the transverse  
52 directions (radial and tangential) but are different in the axial direction. Others have made the more  
53 general assumption of orthotropy (Ashman et al., 1984; Hoffmeister et al., 2000; Rho, 1996) (with  
54 three perpendicular planes of symmetry), where nine elastic coefficients are needed to fully  
55 characterize the medium.

56 Little reference data is available on young bone mechanical behavior, especially on children's  
57 cortical bone. Several papers study mechanical properties of children's bone by uniaxial bending  
58 (Currey and Butler, 1975; Jans et al., 1998; Davis et al., 2012; Agnew et al., 2013; Berteau et al.,  
59 2013; C. I. Albert et al., 2013; Albert et al., 2014), compression (McPherson et al., 2007; Ohman et al.,  
60 2011) or ultrasonic characterization (Berteau et al., 2012, 2013). Some even study mechanical  
61 properties at the tissue level by nanoindentation (Fan et al., 2006; Weber et al., 2006; C. Albert et al.,  
62 2013; Imbert et al., 2014). However, most of these studies were conducted on only a few samples,  
63 because of the scarcity of specimens for laboratory testing. Moreover, the representativeness of these  
64 samples is questionable, since they are largely associated with child pathologies. Due to the limited  
65 number of samples available, papers have up to now focused on mechanical properties in only one  
66 axis, generally the axial direction. The notion of anisotropy, particularly transverse isotropy or  
67 orthotropy, has rarely been investigated. Only one study on this subject reports orthotropy in  
68 children's bone before ossification (McPherson and Kriewall, 1980). In our study, children's bone  
69 samples were recovered from small surgical bone waste, with exclusion criteria; the only way to  
70 obtain non-pathologic bone samples from children. Yet this adds a difficulty: the specimens have been  
71 cut into very small cubes (~2mm), smaller than those used in a previous study which tested 5mm  
72 samples on Resonant Ultrasound Spectroscopy (RUS) and obtained promising results (Bernard et al.,  
73 2013).

74 Here, we report measurements of ultrasonic wave velocities (compressional and shear) in the three  
75 orthogonal bone axes (axial, radial and tangential) to obtain the diagonal elements of the stiffness

76 matrix ( $C_{11}$ ,  $C_{22}$ , etc.). To our knowledge, this study is the first to provide numerous stiffness  
77 coefficients on non-pathologic pediatric cortical bone. The major aim of the study was to obtain  
78 stiffness coefficients of children's cortical bone samples, and to analyze the anisotropic Hooke's law  
79 enabling us to explore the anisotropic behavior of child cortical bone. Values from children were  
80 compared with those from elderly adult cortical bone samples to evaluate how stiffness evolves with  
81 age. To achieve this objective, we required an experimental protocol specifically for measuring  
82 ultrasonic parameters with very small samples, both compressional and shear; the protocol needed to  
83 be reproducible and robust.

84

## 85 **2. Methods**

### 86 **2.1. Sample preparation**

87 15 fibula and 7 femur samples from 21 children (1-18 years old, mean age:  $9.7 \pm 5.8$  years old)  
88 were extracted from surgical waste during lower limb lengthening surgery performed in Marseille,  
89 France. Samples were extracted from the lower 1/3 of the bone. The selected population was  
90 composed of walking children not on drugs disturbing their bone metabolism.

91 16 fibula samples from 16 elderly patients (50-95 years old, mean age:  $76.2 \pm 13.5$  years old) were  
92 extracted from the same anatomic location, but from cadavers at Inserm U1033 and UMR-T 9406  
93 Ifsttar/UCBL (Lyon, France) bone bank.

94 The fresh material was frozen and stored, the child bone at  $-80^{\circ}\text{C}$  (to lessen the impact of collagen  
95 degradation, which will be analyzed in a future study) and the adult bone at  $-20^{\circ}\text{C}$ . The samples were  
96 slowly thawed and then cut with a water-cooled low-speed diamond saw (Buehler Isomet 4000,  
97 Buehler, Lake Bluff, IL, USA) into cubic parallelepipeds (dimensions:  $2 \times 2 \times 2 \text{mm}^3$ ; mean =  $1.96 \pm$   
98  $0.56 \text{mm}$ ). The faces of the specimens were oriented according to the radial (axis 1), tangential (axis 2)  
99 and axial (axis 3) directions defined by the anatomic shape of the bone diaphysis (Figure 1).

100 The greatest challenge here was the very small size of the surgical waste bone (less than 1cm in  
101 the axial axis), the radial thickness of the sample being imposed by the cortical thickness taken. The  
102 second difficulty was cutting samples this small with parallel faces. This necessitated an enhanced  
103 mounting protocol for the cutting. The mass density ( $\rho$ ,  $\text{g/cm}^3$ ) was measured with a micrometric  
104 balance equipped with a density kit (Voyager 610, Ohaus Corporation, FlorhamPark, NJ, USA,  
105 measurement uncertainty of  $0.001 \text{g/cm}^3$ ) and the dimensions were measured with a digital caliper  
106 (Absolute digimatik solar, Mitutoyo, Kanagawa, Japan, measurement error of 0.03 mm).

107

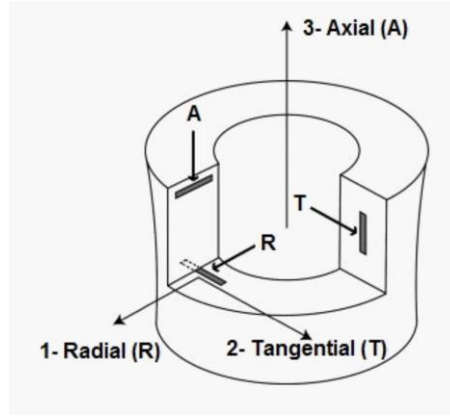


Figure 1: Sketch showing orientation of cortical bone samples prepared to study bone anisotropy. Figure adapted from (Reilly et al., 1974).

## 2.2. Theoretical approach

In this study, we considered cortical human bone as an elastic unlimited medium (the wavelength is smaller than the transverse dimension of the sample). Human bones are generally considered to be orthotropic (Ashman et al., 1984; Yoon and Katz, 1976).

For generally anisotropic media, Hooke's law is written as follows:

$$\sigma_{ij} = C_{ijkl} \varepsilon_{kl} \text{ where } i, j, k, l \in \{1, 2, 3\} \quad (1)$$

In Equation 1,  $\sigma_{ij}$  denotes the  $ij$  component of the stress tensor,  $\varepsilon_{kl}$  represents the components of the strain infinitesimal tensor and  $C_{ijkl}$  is the stiffness tensor. Assuming orthotropic behavior of the bone requires nine independent elastic coefficients of the stiffness tensor which can be expressed in Voigt notation as follows:

$$C_{IJ} = \begin{bmatrix} C_{11} & C_{12} & C_{13} & 0 & 0 & 0 \\ C_{21} & C_{22} & C_{23} & 0 & 0 & 0 \\ C_{31} & C_{32} & C_{33} & 0 & 0 & 0 \\ 0 & 0 & 0 & C_{44} & 0 & 0 \\ 0 & 0 & 0 & 0 & C_{55} & 0 \\ 0 & 0 & 0 & 0 & 0 & C_{66} \end{bmatrix} \quad (2)$$

We calculated the velocities of pure compressional and shear waves propagating along the three principal axes, which gave us the diagonal elements of the stiffness matrix. The relationships between the velocities and elastic coefficients of the material are:

$$\begin{aligned} C_{11} &= \rho V_{11}^2 \\ C_{22} &= \rho V_{22}^2 \\ C_{33} &= \rho V_{33}^2 \\ C_{44} &= \rho V_{23}^2 = \rho V_{32}^2 \\ C_{55} &= \rho V_{13}^2 = \rho V_{31}^2 \\ C_{66} &= \rho V_{12}^2 = \rho V_{21}^2 \end{aligned} \quad (3)$$

$V_{ii}$ : velocity of a compressional wave propagating in the  $i$  direction, with particle motion in the  $i$  direction;

$V_{ij}$ : velocity of a shear wave propagating in the  $i$  direction, with particle motion in the  $j$  direction;

127 Anisotropy was measured as the ratio of elastic constants in the axial/radial ( $C_{33}/C_{11}$ ), in the  
 128 axial/tangential ( $C_{33}/C_{22}$ ) and in the radial/tangential ( $C_{11}/C_{22}$ ) anatomic specimen axes (Rudy et al.,  
 129 2011; Baumann et al., 2012).

130

### 131 2.3. Ultrasonic measurements

132 To find the diagonal elements of the stiffness matrix, the velocities of compressional and shear  
 133 waves need to be determined. Two mountings, one for compressional waves and the other for shear  
 134 waves, were used. For both compressional and shear waves, we assumed a non-dispersive medium and  
 135 we determined the wave velocity propagating in the  $x_i$  direction using a comparison method:

$$V_{ij} = \frac{l_{sample\_i}}{-\Delta t + \frac{l_{ref}}{V_{ref}}}$$

136  $V_{ij}$  : compressional ( $i=j$ ) or shear ( $i \neq j$ ) wave velocity;

137  $l_{sample\_i}$  : thickness of the sample in direction  $x_i$ ;

138  $\Delta t$ : time delay between the first arriving signal travelling in the reference medium and the first  
 139 arriving signal propagating through the bone sample;

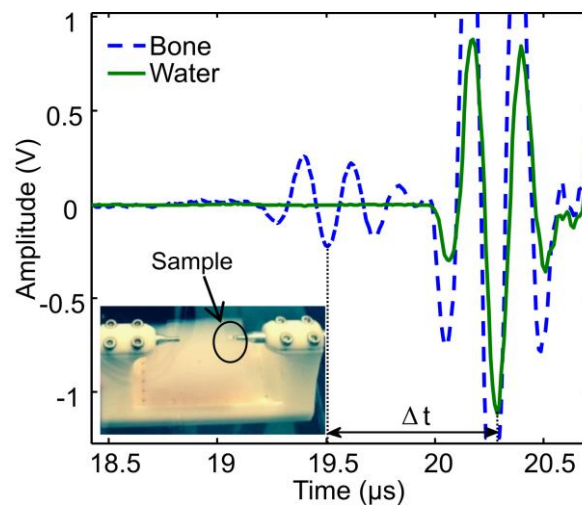
140  $l_{ref}$  : distance between the two transducers in the reference medium;

141  $V_{ref}$  : ultrasonic wave velocity in the reference medium.

142

#### 143 2.3.1. Compressional wave velocity measurement

144 The ultrasonic bench consisted of two transducers (VP1093, center frequency 5MHz, CTS Valpey  
 145 Corporation, Hopkinton, MA) facing each other with their axes aligned and operating in transmission  
 146 mode. The whole device was immersed in water. First, a reference measurement was made in water  
 147 without samples ( $V_{ref}$ ). The bone sample to be tested was then placed over a gelatin block (agar) to  
 148 keep it aligned between the transducers (Figure 2).



149

Figure 2: Picture of the experimental set-up (left), and example of a reference signal (water) and ultrasonic wave through the bone sample.

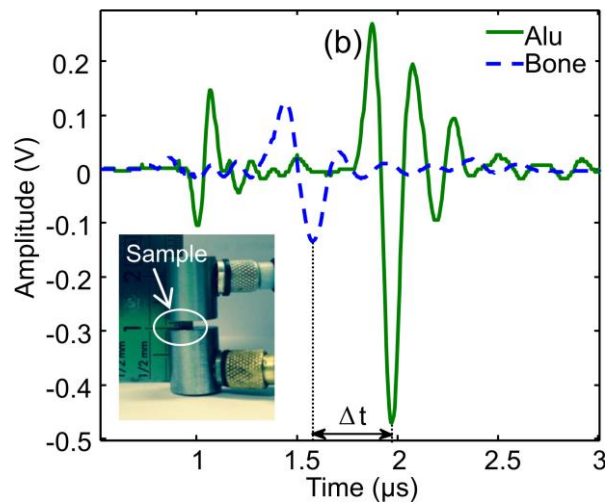
150 The entire protocol was validated on bovine bone samples. We obtained  $V_{11} = 3375 \pm 65$  m/s,  $V_{22} =$   
151  $3637 \pm 91$  m/s and  $V_{33} = 3999 \pm 31$  m/s, in agreement with the literature (Lees et al., 1979; Lipson and  
152 Katz, 1984; Lasaygues and Pithioux, 2002).

153

### 154 2.3.2. Shear wave velocity measurement

155 Measurements were made with two transverse wave transducers (Panametrics V156, 5MHz, Inc.,  
156 Waltham, MA) facing each other with their axes aligned and operating in transmission mode. First, a  
157 reference measurement was made in a 5 mm thick aluminum sample. The bone samples to be tested  
158 were then placed in contact between the transducers (Figure 3).

159



160

Figure 3: Picture of the experimental set-up (left), and example of a reference signal (aluminum sample) and ultrasonic wave through the bone sample.

161

### 162 2.4. Statistical analysis

163 Statistical analysis was performed using the SPSS program (SPSS Statistics 22, IBM, USA). The  
164 Shapiro–Wilk test was used to evaluate the normality of the distribution. A Pearson correlation was  
165 performed for normal distribution and a Spearman correlation was performed for non-normal  
166 distribution. The significance level is  $p < 0.05$ . The Wilcoxon rank-sum test was used to determine the  
167 difference between coefficients.

168

### 169 3. Results

170 Raw data are presented. All the values of ultrasonic wave velocities are given in Table 1, with mean  
171 and standard deviation for each group. The relationships established above between the velocities and  
172 the stiffness coefficients of the material gave the  $C_{ii}$  coefficients summarized in Table 2. The mean  
173 values of elastic coefficients from our study are also compared with values from the literature (Table  
174 2).

175 The elastic coefficients for adult fibulae are quite similar to those from the literature for femur and  
176 tibiae evaluated with ultrasonic methods (Ashman et al., 1984; Hoffmeister et al., 2000). Values from  
177 the children's bone, especially the femur, are lower than those from the adults. Due to the mean age  
178 gap of the two groups (resp.  $12.9 \pm 3.3$  y.o for fibula and  $3.6 \pm 5.3$  y.o for femur), we cannot compare  
179 fibula and femur values in these children. A significant correlation was found in the children's bone  
180 between all the stiffness coefficients and age ( $R > 0.56$ ,  $p < 0.01$ ). Moreover, the stiffness coefficients are  
181 all correlated ( $R > 0.55$ ,  $p < 0.01$ ). In the elderly adult bone, we only found a negative correlation  
182 between  $C_{33}$  and age ( $R = -0.63$ ,  $p < 0.01$ ).

183 No significant difference was found between  $C_{11}$  and  $C_{22}$  and between  $C_{44}$  and  $C_{55}$ , for either adult or  
184 child bone ( $p > 0.5$ ), which confirms transverse isotropy with  $C_{33} > C_{22} = C_{11} > C_{44} = C_{55} > C_{66}$ . In both  
185 groups, we found no correlation between age and anisotropy ratios.

186 Figure 4 shows the evolution of stiffness coefficients with age, revealing that stiffness coefficients  
187 increase in growing bone. Moreover, the effect of main direction is observed, with the axial stiffness  
188 coefficient ( $C_{33}$ ) 1/3 above radial and tangential values (respectively  $C_{11}$  and  $C_{22}$ ).

189 Figure 5 illustrates the evolution of the axial stiffness coefficient ( $C_{33}$ ) with age. Depending on age  
190 range, the linear interpolation slope changes from positive to negative. A Spearman correlation was  
191 found between age and  $C_{33}$ ; in the children's bone, we obtained a positive value ( $R = 0.694$ ,  $p < 0.01$ )  
192 whereas in the elderly adult bone, we obtained a negative value ( $R = -0.634$ ,  $p = 0.08$ ).

193 Figure 6 represents the evolution of anisotropy ratios with age. In both groups, we found no  
194 correlation between age and anisotropy ratios.

195  
196  
197  
198  
199  
200  
201  
202  
203  
204  
205  
206  
207  
208  
209  
210  
211



212 Table 1. Ultrasonic wave velocities (compressional and shear) for all directions

Samples	Age years	Mass density kg/m <sup>3</sup>	V <sub>11</sub> m/s	V <sub>22</sub> m/s	V <sub>33</sub> m/s	V <sub>31</sub> m/s	V <sub>32</sub> m/s	V <sub>13</sub> m/s	V <sub>12</sub> m/s	V <sub>23</sub> m/s	V <sub>21</sub> m/s
fibula 1	6	1873	2924	2912	3632	1506	1553	1446	1279	1535	1340
fibula 2*	10	1864	2972	2537	3596	1603	1701	1525	1306	1598	1378
fibula 3	10	1398	2406	2449	2920	1309	1347	1435	1339	1248	1460
fibula 4	10	1768	3170	3137	3994	1621	1608	1628	1354	1613	1379
fibula 5	10	1690	3181	2836	3358	1462	1409	1459	1361	1501	1202
fibula 6	12	1735	3033	3069	3873	1615	1591	1549	1355	1547	1431
fibula 7	13	1664	3053	3155	3491	1351	1514	1471	1319	1526	1243
fibula 8	14	1598	3194	2728	3320	1314	1348	1462	1165	1280	1199
fibula 9	14	1790	3228	3031	3964	1520	1616	1352	1478	1444	1269
fibula 10	15	1848	2985	3183	3918	1608	1599	1628	1369	1664	1295
fibula 11	15	1798	3099	3166	3666	1548	1551	1540	1347	1584	1365
fibula 12	16	1882	3199	3100	4057	1662	1612	1737	1436	1557	1329
fibula 13	17	1617	3455	3566	4012	1525	1616	1583	1364	1666	1396
fibula 14	18	1764	3071	3103	3918	1641	1684	1489	1440	1651	1351
<b>Mean</b>	<b>12.9</b>	<b>1734</b>	<b>2930</b>	<b>2903</b>	<b>1466</b>	<b>1507</b>	<b>1475</b>	<b>1324</b>	<b>1500</b>	<b>1303</b>	<b>1466</b>
<b>SD</b>	<b>3.3</b>	<b>182</b>	<b>292</b>	<b>279</b>	<b>132</b>	<b>121</b>	<b>120</b>	<b>99</b>	<b>116</b>	<b>89</b>	<b>132</b>
femur 1	1	1498	2491	2532	2960	1307	1362	1343	1272	1440	1383
femur 2	1	1712	2791	2798	3146	1287	1494	1404	1113	1464	1224
femur 3	1	1365	2515	2616	3206	1314	1319	1217	1209	1393	1250
femur 4	1	1873	2751	2858	3132	1403	1479	1314	1213	1505	1255
femur 5	1	1688	2678	2654	3287	1398	1383	1375	1220	1400	1154
femur 6	5	1798	2892	2658	3642	1298	1341	1477	1475	1378	1147
femur 7	15	2197	2439	2883	3613	1500	1520	1552	1397	1503	1315
<b>Mean</b>	<b>3.57</b>	<b>1733</b>	<b>2651</b>	<b>2714</b>	<b>3284</b>	<b>1358</b>	<b>1414</b>	<b>1383</b>	<b>1271</b>	<b>1440</b>	<b>1247</b>
<b>SD</b>	<b>5.26</b>	<b>268</b>	<b>172</b>	<b>133</b>	<b>255</b>	<b>79</b>	<b>81</b>	<b>109</b>	<b>124</b>	<b>52</b>	<b>84</b>
Adult 1	67	1748	4258	3190	3382	1599	1707	1645	1385	1618	1399
Adult 2	80	1761	4028	3390	3556	1586	1626	1636	1454	1621	1431
Adult 3	95	1623	3862	2672	3465	1728	1684	1676	1298	1545	1344
Adult 4	68	1664	4402	3367	3514	1727	1732	1679	1426	1705	1421
Adult 5	87	1573	3770	2755	2195	2218	1680	1464	1238	1550	1507
Adult 6	83	1798	3818	3412	3169	1575	1658	1690	1386	1600	1412
Adult 7	78	1647	3965	3248	2442	1699	1564	1684	1609	1579	1490
Adult 8	73	1831	3819	3051	2014	1840	1667	1598	1234	1675	1532
Adult 9	73	1855	4011	3332	3375	1660	1627	1661	1394	1662	1404
Adult 10	77	2230	3830	3020	3128	1473	1492	1728	1788	1476	1359

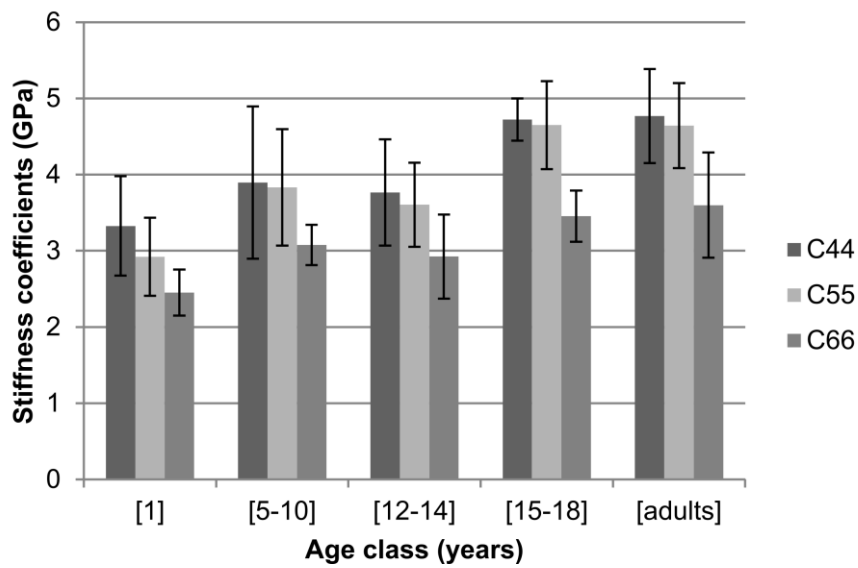
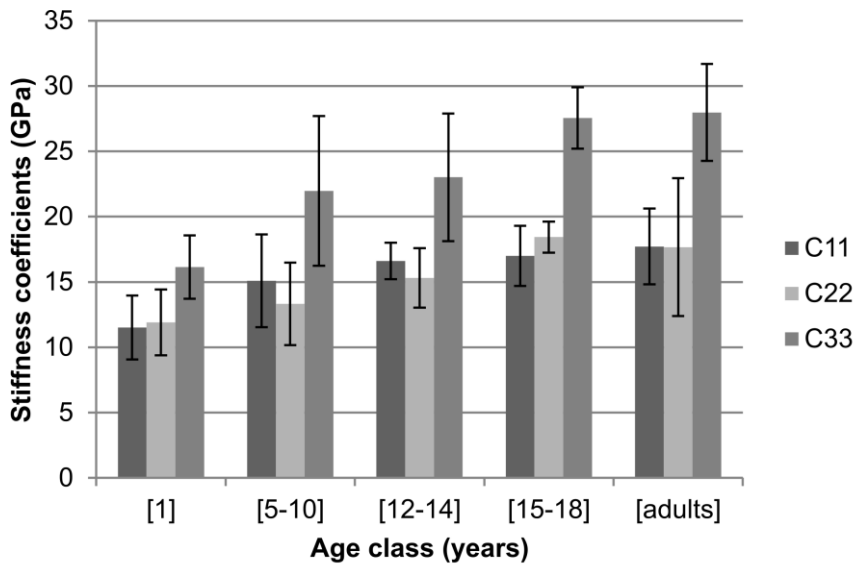
Adult 11	89	1577	3867	3299	3280	1620	1637	1582	1374	1679	1346
Adult 12	50	1775	4071	3414	3508	1645	1713	1714	1398	1691	1381
Adult 13	76	1882	4192	3016	3447	1529	1720	1665	1464	1669	1497
Adult 14	56	1914	4093	3206	3454	1583	1693	1472	1439	1718	1635
Adult 15	91	1498	3906	3166	3068	1368	1602	1617	1434	1559	1328
Adult 16	57	1623	4015	3250	3191	1504	1675	1653	1502	1575	1398
<b>Mean</b>	<b>76.2</b>	<b>1750</b>	<b>3174</b>	<b>3137</b>	<b>3994</b>	<b>1647</b>	<b>1655</b>	<b>1635</b>	<b>1426</b>	<b>1620</b>	<b>1430</b>
<b>SD</b>	<b>13.5</b>	<b>177</b>	<b>223</b>	<b>486</b>	<b>178</b>	<b>189</b>	<b>63</b>	<b>76</b>	<b>134</b>	<b>69</b>	<b>82</b>

213 \* Mean value of two fibulae samples from the same child.

214

215 **Table 2. Average stiffness coefficients (SD)**

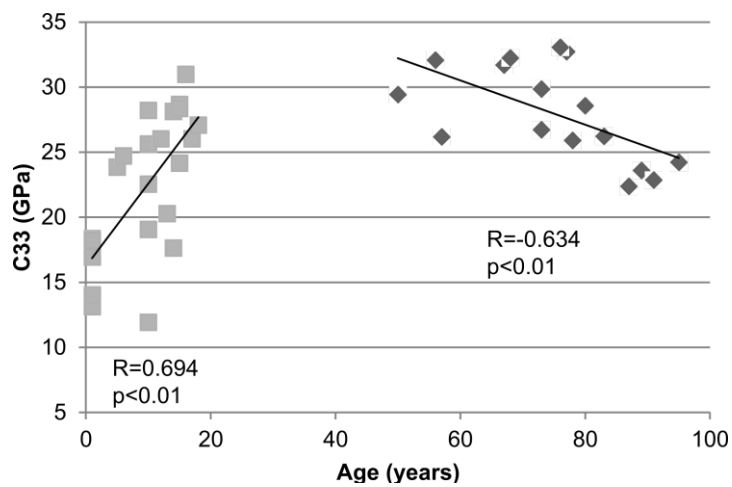
	Children (n=14)	Children (n=7)	Adults (n=16)	Hoffmeister (Hoffmeister et al., 2000)	Ashman (Ashman et al., 1984)
	fibula (GPa)	femur (GPa)	fibula (GPa)	tibia (GPa)	femur (GPa)
C <sub>11</sub>	16.5 (2.70)	12.2 (2.42)	17.7 (2.89)	19.5 (2.0)	18.0 (1.60)
C <sub>22</sub>	15.8 (3.24)	12.9 (3.15)	17.7 (5.27)	20.1 (1.9)	20.2 (1.79)
C <sub>33</sub>	24.0 (5.15)	19.0 (5.50)	28.0 (3.71)	30.9 (2.1)	27.6 (1.74)
C <sub>44</sub>	4.17 (0.800)	3.57 (0.833)	4.69 (0.518)	5.72 (0.49)	6.23 (0.479)
C <sub>55</sub>	4.05 (0.746)	3.31 (0.921)	4.72 (0.579)	5.17 (0.57)	5.61 (0.398)
C <sub>66</sub>	3.13 (0.373)	2.77 (0.656)	3.60 (0.690)	4.05 (0.54)	4.52 (0.371)



216

217 Figure 4: Comparison of the mean ( $\pm$  standard deviation) of the stiffness coefficients with age class

218



219

220 Figure 5: Axial stiffness coefficient measured on children's bone samples (squares) and elderly adults'

221

bone samples (diamonds).

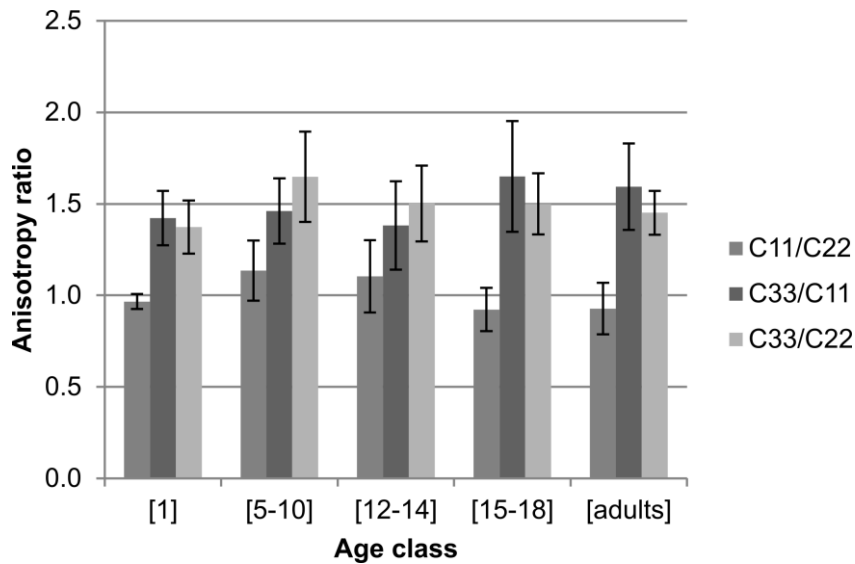


Figure 6: Representation of the mean ( $\pm$  standard deviation) of anisotropy ratios by age class.

#### 4. Discussion

The first aim of the study was to determine and to compare stiffness coefficients in children's and elderly adults' cortical bone samples. The method we used is based on measuring both compressional and shear ultrasonic bulk wave velocities (BWV) propagating along various directions of a bone specimen (Lang, 1969). While this method is widely used, it has major drawbacks related to specimen size and geometry. With a range frequency of 1-2.5 MHz, the specimen must typically be larger than a few millimeters (~5 mm). This is because measured wave velocities must be linked to bulk waves, which propagate when the wavelength is smaller than the dimension of the specimen (Ashman et al., 1984). In this study, samples were machined from fibulae whose cortical thickness was below 3mm. By improving the cutting process so as to avoid any lack of parallelism, we finally obtained specimens of approximately  $2 \times 2 \times 2 \text{ mm}^3$ . For both compressional and shear wave velocity measurements, we used a frequency of 5 MHz to achieve a wavelength greater than the typical size of bone tissue heterogeneities (< a few hundred microns) and smaller than the specimen dimensions. Another limitation of this study was that only elastic constants for the main diagonal of the stiffness tensor could be evaluated. It takes one or several  $45^\circ$  oblique cuts to retrieve all non-diagonal terms of the stiffness tensor, which was not technically possible with our specimen size. This prevented conversion of the elastic stiffness coefficients into engineering coefficients (Young's moduli, shear moduli and Poisson's ratios).

The longitudinal stiffness coefficients ( $C_{11}$ ,  $C_{22}$  and  $C_{33}$ ) generally found for adult cortical bone with the ultrasonic method range between 16.8 GPa and 31.7 GPa (Ashman et al., 1984; Bernard et al., 2013; Espinoza Orías et al., 2009; Hoffmeister et al., 2000). However, these values were for femur or tibia bone; to our knowledge, no value for the fibula is available. These results on adult fibulae therefore contribute a new batch of data and allow us to compare adults' and children's values for the same bone from the same anatomic location. The results on children's bone enrich the literature

249 concerning the mechanical properties of children's bone. Our findings show that stiffness coefficients  
250 increase with age up to puberty, when they appear to reach adult values (Figure 4). The evolution of  
251  $C_{33}$  with age shows a linear regression by age group, positive in the children and negative in the adults  
252 (Figure 5). This trend is similar to the evolution of the bone mineral density with age (Bonjour, 1998;  
253 Boot et al., 2010). An *in vivo* study by Drozdowska et al. (Drozdowska and Pluskiewicz, 2003)  
254 assessed the speed of sound (SOS) at the hand phalanx in a population of people aged from 7 to 80.  
255 The authors conclude that the SOS increases linearly to a maximum reached at around 25-30 years  
256 old, after which values decrease more slowly up to the age of 80. These data differ from ours because  
257 the *in vivo* approach introduces the effect of soft tissue and bone geometry. Moreover, the study was  
258 performed on the hand phalanx, which is not mechanically stressed. Nevertheless, even with the gap in  
259 age coverage between our studies (our population being children of 1-18 and adults of 50-95), our *in*  
260 *vitro* results exhibit the same trend as their *in vivo* study.

261 The second aim of this study was to analyze the anisotropic behavior of our samples. The results  
262 for all specimens show transverse isotropy for both adult and child bone, and both fibula and femur, at  
263 the location tested. Several studies point to the fact that ultrasonic wave velocity measurement relies  
264 on anatomical location. It has been suggested that ultrasonic wave velocity depends on the  
265 circumferential location (Bensamoun et al., 2004; Rho, 1996). Rudy et al. showed that anisotropy  
266 depends on the location along the bone: their tissue specimens, pooled from multiple donors, exhibited  
267 orthotropy at all locations along the femoral diaphysis and transverse isotropy at mid-diaphysis (Rudy  
268 et al., 2011). In this study, samples were extracted from the lower 1/3 of the bone, which does not  
269 explain the transverse isotropy.

270 Anisotropy in cortical bone can be explained by multiple factors. Bone material properties depend  
271 on microscopic-scale components such as hydroxyapatite crystals and collagen (Hasegawa et al.,  
272 1994; Burr, 2002; Currey, 2003; Follet, 2004; Boivin et al., 2008), and their layout, as confirmed  
273 experimentally in a study showing that ultrasonic velocity is influenced by changes in organic matrix  
274 (Mehta et al., 1998). Katz et al. argued that orthotropic versus transversely isotropic symmetry was  
275 dependent on whether the tissue exhibited a predominately laminar or Haversian microstructure,  
276 respectively (Katz et al., 1984). According to Baumann et al., transverse isotropy is governed  
277 primarily by apatite crystal orientations while orthotropy is governed primarily by intracortical  
278 porosity (Baumann et al., 2012). While our study did not investigate any of these factors, further  
279 exploration would enrich our knowledge of the anisotropy of bone.

280 In conclusion, this study contributes a new set of ultrasonic wave velocities and elasticity values for  
281 children's cortical bone, providing insights into the evolution of stiffness coefficients with age.  
282 Moreover, it offers the first complete analysis of stiffness coefficients in the three orthogonal bone  
283 axes in children, giving some indication of how bone anisotropy is related to age. Future perspectives  
284 include studying the effect of the structure and composition of bone on its mechanical behavior.

285

286 **Acknowledgments**

287 This research is supported by the French National Research Agency (ANR MALICE Program,  
288 under Grant No. BS09-032). We thank the Timone Hospital surgery team and the donors or their legal  
289 guardians who gave informed written consent to providing their tissues for investigation, in  
290 accordance with the French Code of Public Health (Code de la Santé Publique Française) and  
291 approved by the Committee for the Protection of Persons. This work has benefited from the help of  
292 Marine LOUBET for the setting up of experiments. We thank Marjorie SWEETKO for English  
293 language revision.

294

295 **References**

- 296 Agnew, A.M., Moorhouse, K., Kang, Y.-S., Donnelly, B.R., Pfefferle, K., Manning, A.X., Litsky,  
297 A.S., Herriott, R., Abdel-Rasoul, M., Bolte, J.H., 2013. The Response of Pediatric Ribs to  
298 Quasi-static Loading: Mechanical Properties and Microstructure. *Ann. Biomed. Eng.* 41,  
299 2501–2514. doi:10.1007/s10439-013-0875-6
- 300 Albert, C.I., Jameson, J., Harris, G., 2013. Design and validation of bending test method for  
301 characterization of miniature pediatric cortical bone specimens. *Proc. Inst. Mech. Eng. [H]*  
302 227, 105–113.
- 303 Albert, C., Jameson, J., Smith, P., Harris, G., 2014. Reduced diaphyseal strength associated with high  
304 intracortical vascular porosity within long bones of children with osteogenesis imperfecta.  
305 *Bone* 66, 121–130. doi:10.1016/j.bone.2014.05.022
- 306 Albert, C., Jameson, J., Toth, J.M., Smith, P., Harris, G., 2013. Bone properties by nanoindentation in  
307 mild and severe osteogenesis imperfecta. *Clin. Biomech.* 28, 110–116.  
308 doi:10.1016/j.clinbiomech.2012.10.003
- 309 Ashman, R.B., Cowin, S.C., Van Buskirk, W.C., Rice, J.C., 1984. A continuous wave technique for  
310 the measurement of the elastic properties of cortical bone. *J. Biomech.* 17, 349–361.  
311 doi:10.1016/0021-9290(84)90029-0
- 312 Baumann, A.P., Deuring, J.M., Rudy, D.J., Niebur, G.L., Roeder, R.K., 2012. The relative influence  
313 of apatite crystal orientations and intracortical porosity on the elastic anisotropy of human  
314 cortical bone. *J. Biomech.* 45, 2743–2749. doi:10.1016/j.jbiomech.2012.09.011
- 315 Bensamoun, S., Ho Ba Tho, M.-C., Luu, S., Gherbezza, J.-M., de Belleval, J.-F., 2004. Spatial  
316 distribution of acoustic and elastic properties of human femoral cortical bone. *J. Biomech.* 37,  
317 503–510. doi:10.1016/j.jbiomech.2003.09.013
- 318 Bernard, S., Grimal, Q., Laugier, P., 2013. Accurate measurement of cortical bone elasticity tensor  
319 with resonant ultrasound spectroscopy. *J. Mech. Behav. Biomed. Mater.*  
320 doi:10.1016/j.jmbbm.2012.09.017
- 321 Berteau, J.-P., Baron, C., Pithioux, M., Launay, F., Chabrand, P., Lasaygues, P., 2013. In vitro  
322 ultrasonic and mechanic characterization of the modulus of elasticity of children cortical bone.  
323 *Ultrasonics*. doi:10.1016/j.ultras.2013.09.014
- 324 Berteau, J.-P., Pithioux, M., Follet, H., Guivier-Curien, C., Lasaygues, P., Chabrand, P., 2012.  
325 Computed tomography, histological and ultrasonic measurements of adolescent scoliotic rib  
326 hump geometrical and material properties. *J. Biomech.* 45, 2467–2471.  
327 doi:10.1016/j.jbiomech.2012.07.002
- 328 Boivin, G., Bala, Y., Doublier, A., Farlay, D., Ste-Marie, L.G., Meunier, P.J., Delmas, P.D., 2008. The  
329 role of mineralization and organic matrix in the microhardness of bone tissue from controls  
330 and osteoporotic patients. *Bone* 43, 532–538. doi:10.1016/j.bone.2008.05.024
- 331 Bonjour, J.P., 1998. Delayed puberty and peak bone mass. *Eur. J. Endocrinol.* 139, 257–259.  
332 doi:10.1530/eje.0.1390257
- 333 Boot, A.M., de Ridder, M.A.J., van der Sluis, I.M., van Slobbe, I., Krenning, E.P., Keizer-Schrama,  
334 S.M.P.F. de M., 2010. Peak bone mineral density, lean body mass and fractures. *Bone* 46,  
335 336–341. doi:10.1016/j.bone.2009.10.003

336 Burr, D.B., 2002. The contribution of the organic matrix to bone's material properties. *Bone* 31, 8–11.

337 Choi, K., Kuhn, J.L., Ciarelli, M.J., Goldstein, S.A., 1990. The elastic moduli of human subchondral,

338 trabecular, and cortical bone tissue and the size-dependency of cortical bone modulus. *J.*

339 *Biomech.* 23, 1103–1113.

340 Cuppone, M., Seedhom, B.B., Berry, E., Ostell, A.E., 2004. The longitudinal Young's modulus of

341 cortical bone in the midshaft of human femur and its correlation with CT scanning data.

342 *Calcif. Tissue Int.* 74, 302–309. doi:10.1007/s00223-002-2123-1

343 Currey, J.D., 2003. Role of collagen and other organics in the mechanical properties of bone.

344 *Osteoporos. Int.* 14, 29–36. doi:10.1007/s00198-003-1470-8

345 Currey, J.D., Butler, G., 1975. The mechanical properties of bone tissue in children. *J. Bone Joint*

346 *Surg. Am.* 57, 810–814.

347 Davis, M.T., Loyd, A.M., Shen, H.H., Mulroy, M.H., Nightingale, R.W., Myers, B.S., Bass, C.D.,

348 2012. The mechanical and morphological properties of 6 year-old cranial bone. *J. Biomech.*

349 45, 2493–2498. doi:10.1016/j.jbiomech.2012.07.001

350 Drozdowska, B., Pluskiewicz, W., 2003. Skeletal status in males aged 7-80 years assessed by

351 quantitative ultrasound at the hand phalanges. *Osteoporos. Int.* 14, 295–300.

352 doi:10.1007/s00198-002-1355-2

353 Espinoza Orías, A.A., Deuerling, J.M., Landrigan, M.D., Renaud, J.E., Roeder, R.K., 2009. Anatomic

354 variation in the elastic anisotropy of cortical bone tissue in the human femur. *J. Mech. Behav.*

355 *Biomed. Mater.* 2, 255–263. doi:10.1016/j.jmbbm.2008.08.005

356 Fan, Z., Smith, P.A., Eckstein, E.C., Harris, G.F., 2006. Mechanical properties of OI type III bone

357 tissue measured by nanoindentation. *J. Biomed. Mater. Res. A* 79A, 71–77.

358 doi:10.1002/jbm.a.30713

359 Follet, H., 2004. The degree of mineralization is a determinant of bone strength: a study on human

360 calcanei. *Bone* 34, 783–9. doi:10.1016/j.bone.2003.12.012

361 Grimal, Q., Hauptert, S., Mitton, D., Vastel, L., Laugier, P., 2009. Assessment of cortical bone

362 elasticity and strength: Mechanical testing and ultrasound provide complementary data. *Med.*

363 *Eng. Phys.* 31, 1140–1147. doi:10.1016/j.medengphy.2009.07.011

364 Haïat, G., Naili, S., Grimal, Q., Talmant, M., Desceliers, C., Soize, C., 2009. Influence of a gradient of

365 material properties on ultrasonic wave propagation in cortical bone: application to axial

366 transmission. *J. Acoust. Soc. Am.* 125, 4043–4052. doi:10.1121/1.3117445

367 Hasegawa, K., Turner, C.H., Burr, D.B., 1994. Contribution of collagen and mineral to the elastic

368 anisotropy of bone. *Calcif. Tissue Int.* 55, 381–386. doi:10.1007/BF00299319

369 Ho Ba Tho, M.-C., Rho, J.Y., Ashman, R.B., 1991. Atlas of mechanical properties of human cortical

370 and cancellous bone.

371 Hoffmeister, B.K., Smith, S.R., Handley, S.M., Rho, J.Y., 2000. Anisotropy of Young's modulus of

372 human tibial cortical bone. *Med. Biol. Eng. Comput.* 38, 333–338.

373 Imbert, L., Aurégan, J.-C., Pernelle, K., Hoc, T., 2014. Mechanical and mineral properties of

374 osteogenesis imperfecta human bones at the tissue level. *Bone* 65, 18–24.

375 doi:10.1016/j.bone.2014.04.030

376 Jans, G., Van Audekercke, R., Sloten, J.V., Gobin, R., Van der Perre, G., Mommaerts, M.Y., 1998.

377 P020 Bending properties of cranial bone segments of new-born children. *J. Biomech.* 31,

378 Supplement 1, 65. doi:10.1016/S0021-9290(98)80132-2

379 Katz, J.L., Yoon, H.S., Lipson, S., Maharidge, R., Meunier, A., Christel, P., 1984. The effects of

380 remodeling on the elastic properties of bone. *Calcif. Tissue Int.* 36 Suppl 1, S31–36.

381 Keller, T.S., Mao, Z., Spengler, D.M., 1990. Young's modulus, bending strength, and tissue physical

382 properties of human compact bone. *J. Orthop. Res. Off. Publ. Orthop. Res. Soc.* 8, 592–603.

383 doi:10.1002/jor.1100080416

384 Lang, S.B., 1969. Elastic coefficients of animal bone. *Science* 165, 287–288.

385 Lasaygues, P., Pithioux, M., 2002. Ultrasonic characterization of orthotropic elastic bovine bones.

386 *Ultrasonics* 39, 567–573. doi:10.1016/S0041-624X(02)00261-5

387 Lees, S., Heeley, J.D., Cleary, P.F., 1979. A study of some properties of a sample of bovine cortical

388 bone using ultrasound. *Calcif. Tissue Int.* 29, 107–117.

389 Lipson, S.F., Katz, J.L., 1984. The relationship between elastic properties and microstructure of

390 bovine cortical bone. *J. Biomech.* 17, 231–240.

391 Lotz, J.C., Gerhart, T.N., Hayes, W.C., 1991. Mechanical properties of metaphyseal bone in the  
392 proximal femur. *J. Biomech.* 24, 317–329. doi:10.1016/0021-9290(91)90350-V

393 McPherson, G.K., Kriewall, T.J., 1980. Fetal head molding: An investigation utilizing a finite element  
394 model of the fetal parietal bone. *J. Biomech.* 13, 17–26. doi:10.1016/0021-9290(80)90004-4

395 McPherson, S.B.I., Copley, L.A.B., Niemann, J.J., Lankachandra, K., Williams, J.L., 2007.  
396 Biomechanical evaluation of fetal calf skull as a model for testing halo-pin designs for use in  
397 children. *J. Biomech.* 40, 1137–1144. doi:10.1016/j.jbiomech.2006.05.003

398 Mehta, S.S., Oz, O.K., Antich, P.P., 1998. Bone elasticity and ultrasound velocity are affected by  
399 subtle changes in the organic matrix. *J. Bone Miner. Res. Off. J. Am. Soc. Bone Miner. Res.*  
400 13, 114–121. doi:10.1359/jbmr.1998.13.1.114

401 Neil Dong, X., Edward Guo, X., 2004. The dependence of transversely isotropic elasticity of human  
402 femoral cortical bone on porosity. *J. Biomech.* 37, 1281–1287.  
403 doi:10.1016/j.jbiomech.2003.12.011

404 Ohman, C., Baleani, M., Pani, C., Taddei, F., Alberghini, M., Viceconti, M., Manfrini, M., 2011.  
405 Compressive behaviour of child and adult cortical bone. *Bone* 49, 769–776.  
406 doi:10.1016/j.bone.2011.06.035

407 Reilly, D.T., Burstein, A.H., 1975. The elastic and ultimate properties of compact bone tissue. *J.*  
408 *Biomech.* 8, 393–405. doi:10.1016/0021-9290(75)90075-5

409 Reilly, D.T., Burstein, A.H., Frankel, V.H., 1974. The elastic modulus for bone. *J. Biomech.* 7, 271–  
410 275. doi:10.1016/0021-9290(74)90018-9

411 Rho, J.-Y., 1996. An ultrasonic method for measuring the elastic properties of human tibial cortical  
412 and cancellous bone. *Ultrasonics* 34, 777–783. doi:10.1016/S0041-624X(96)00078-9

413 Rudy, D.J., Deuerling, J.M., Espinoza Orías, A.A., Roeder, R.K., 2011. Anatomic variation in the  
414 elastic inhomogeneity and anisotropy of human femoral cortical bone tissue is consistent  
415 across multiple donors. *J. Biomech.* 44, 1817–1820. doi:10.1016/j.jbiomech.2011.04.009

416 Smith, C.B., Smith, D.A., 1976. Relations between age, mineral density and mechanical properties of  
417 human femoral compacta. *Acta Orthop.* 47, 496–502.

418 Weber, M., Roschger, P., Fratzl-Zelman, N., Schöberl, T., Rauch, F., Glorieux, F.H., Fratzl, P.,  
419 Klaushofer, K., 2006. Pamidronate does not adversely affect bone intrinsic material properties  
420 in children with osteogenesis imperfecta. *Bone* 39, 616–622. doi:10.1016/j.bone.2006.02.071

421 Yoon, H.S., Katz, L.J., 1976. Ultrasonic wave propagation in human cortical bone—II. Measurements  
422 of elastic properties and microhardness. *J. Biomech.* 9, 459–464. doi:10.1016/0021-  
423 9290(76)90089-0

424 Zioupos, P., Currey, J., 1998. Changes in the Stiffness, Strength, and Toughness of Human Cortical  
425 Bone With Age. *Bone* 22, 57–66. doi:10.1016/S8756-3282(97)00228-7

426